Semiempirical Methods for Systematization of High-Precision Atomic Data

Recent experimental advances have made possible spectroscopic measurements of unprecedented precision for highly excited, highly ionized, and highly complex atomic systems. The accuracies involved often exceed theoretical capabilities and semiempirical methods have been useful in the interpretation of results. Systematizations of data have been achieved through refinements and extensions of traditional semiempirical methods such as quantum defect analyses, core polarization formulations, and screening parametrizations. In some cases unexpected regularities have been revealed that not only permit accurate extrapolative predictions, but also pose challenges to ab initio theory.

INTRODUCTION

The long and successful history of atomic spectroscopy has proceeded primarily through empirical exposition and systematization of diverse data. Empirical approaches were necessitated by the high precision of optical measurements, which often surpassed existing theoretical capabilities. Empirical regularities can be exploited for the prediction and interpretation of experimental measurements, and they often provide insights into the nature of the physical interactions. This trend continues today, particularly in the study of highly excited, highly ionized, and highly complex atoms. Classical spectroscopic light sources have been complemented by magnetically confined and laser-produced plasmas, fast-ion-beam excitation, astrophysical observations and multiple photon excitation processes using lasers, rf

Comments At. Mol. Phys.
1985, Vol. 16, No. 1, pp. 1–19
0010-2687/85/1601-0001/$20.00/0

excitation, and external fields. This has provided large blocks of data, much of unprecedented precision, that can be studied along Rydberg series, yrast or yrare chains, or isoelectronic, isoionic, isonuclear, or homologous sequences. In this context many of the traditional empirical methods such as quantum defect analyses, core polarization formulations, screening parametrizations, and semiclassical modelings have been refined and extended to new regimes with the benefit of modern theoretical concepts. A few recent examples will be described below that not only provide extrapolative and interpolative predictions, but also reveal unexpected regularities that challenge ab initio theory.

QUANTUM DEFECT METHODS

The semiempirical formulation of spectroscopic data began with Rydberg's quantum defect parametrization of the hydrogenic Balmer formula[1]

$$E_{nl} = E_\infty - \mathrm{Ry}\,\zeta^2/(n - \delta_{nl})^2. \tag{1}$$

E_{nl} is the excitation energy for a level with quantum numbers n and l, E_∞ is the ionization energy of the ground state, Ry is the (reduced-mass corrected) Rydberg constant, $\zeta = Z - N + 1$ is the net core charge (Z = nuclear charge and N = number of electrons) and δ_{nl} is the quantum defect that this equation serves to define. For systems that separate into a single active outer electron and a relatively passive core of inner electrons, δ has a smooth and weak dependence upon n described by the Ritz expansion[1]

$$\delta_{nl} = a_l + b_l/(n - \delta_{nl})^2 + c_l/(n - \delta_{nl})^4 + \ldots. \tag{2}$$

Equation (2) is typical of the expansions used in these semiempirical approaches, in that δ_{nl} appears on both sides of the equation and is manipulated by iteration. Though its historic origins were purely empirical, the quantum defect concept can be deduced theoretically from the WKB approximation as a phase shift in the external wavefunction, and the Ritz formula can similarly be derived through an energy expansion.[2]

Spectroscopic determinations of ionization potentials are usually accomplished by least squares adjustment of E_∞ and the Ritz parameters a_l, b_l, c_l, etc. A different set of Ritz parameters must be deduced for each Rydberg series in a given ion and these quantities provide operational definitions for the phenomenological properties of core penetration and core polarization.[3] Deeply penetrating orbits are characterized by a large quantum defect and a positive value for b_l, whereas nonpenetrating orbits have a small (<0.01) quantum defect and a negative value for b_l. Defined in this manner, core penetration generally decreases with increasing Z along an isoelectronic sequence, whereas core polarization passes through an isoelectronic maximum.[1,4]

Laser techniques such as two-photon Doppler-free spectroscopy now permit the determination of the energy levels of high Rydberg states to accuracies within parts in 10^8 [e.g. Ref. 5]. Quantum defect studies have been made[6] for $n > 100$ and observations of Rydberg states of light atoms for $n - 300$ are now routinely made in astronomical radio recombination spectra.[7] Studies of Rydberg atoms in the presence of strong electric and magnetic fields have also provided a powerful means of probing these states.[8]

Although Eq. (1) is used primarily for situations described by the independent electron model, it has been extended to include cases where electron correlations dominate. Systems with two equivalent s electrons outside a core often exhibit correlations along the hyperspherical "Wannier ridge" mode in which the electrons selectively reside on opposing sides of the core. Thus the (unpenetrated) effective charge screening of each equivalent electron by the other is reduced to a fraction of its actual charge. At the Wannier point the theoretical screening becomes ¼ electron charge and the effective screened charge in Eq. (1) would become $\zeta = Z - N + 2 - ¼$. Read[9] has fitted term energies of singly and doubly excited ns^2 configurations to a modified Rydberg formula that doubles Eq. (1) and parametrizes both the screening and the (assumed constant) quantum defect. He found that the fitted screening fraction was generally about 0.257, slightly exceeding the Wannier value.

A comprehensive calculational framework has been developed to treat systems for which the single configuration picture is not valid. Multichannel quantum defect theory[10] and the Lu–Fano diagrammatic method[11] have been used very successfully in cases where a

series is perturbed by an interloping level, or where two or more mutually interacting series converge to differing ionization limits. This approach allows the correlation of large amounts of data in a format that manifestly displays configuration interaction and allows parameters to be determined empirically.

The quantum defect theory also provides predictions for oscillator strengths and related quantities through the Coulomb approximation. Although the method is simple and unsophisticated, there are recent indications that it may actually be superior to existing ab initio methods for applications to alkali-like systems. Since it uses empirical effective quantum numbers, it could conceivably account implicitly for interactions that would require extensive explicit perturbative corrections in an ab initio calculation. A number of relevant recent measurements are presented in Table I, along with calculations by Lindgård and Nielsen[12] using the numerical Coulomb approximation and ab initio calculations. In a high precision lifetime measurement, Gaupp *et al.*[13] determined the oscillator strengths of the lowest resonance transitions in neutral lithium and sodium to within $\pm 0.25\%$. The numerical Coulomb approximation agrees with the Li result to within 0.05% and with the Na result to within 0.7%. Reference 13

TABLE I

Comparison of observed, semiempirical, and ab initio values for oscillator strength related quantities in alkali-like systems (α_d in units a_0^3)

Quantity	Observed	Numerical Coulomb[a]	Ab initio	
$3f$ (Li–Res)	0.7416(12)[b]	0.7412	0.764[c]	
$3f$ (Na–Res)	0.9536(16)[b]	0.9468	0.983[c]	
α_d (Mg^+)	33.0(5)[d]	33.9	38.8[e], 37.2[f]	
α_d (Ca^+)	75.3(4)[g]	74.7	89,[h] 112.5,[e] 96.3[f]	
α_d (Ba^+)	111.8[i]	117.1	144.1[i]	

[a]Lindgard and Nielsen.[12]
[b]Gaupp *et al.*[13]
[c]Average of ab initio calculations cited by Ref. 13.
[d]Chang and Noyes.[45]
[e]Easa and Shukla.[46]
[f]Langhoff and Hurst.[47]
[g]Chang.[42]
[h]Vaidjanathan and Shorer.[41]
[i]Curtis et al.[38]

compiles 45 ab initio theoretical calculations for these two lifetimes: none is within two experimental standard deviations of the experimental result and most exhibit discrepancies of several percent. (Curiously, Ref. 12 was not included in the compilation.) Doubts have been raised[14] that uncertainties in ab initio theoretical calculations can accommodate the discrepancy in the lithium case. The situation demands clarification. Table I also lists recent spectroscopic determinations of alkali-like core polarizabilities in alkaline earth spectra. Here again the Coulomb approximation estimates appear to be superior to ab initio calculations. This will be discussed further in the section on core polarization models.

The quantum defect approach to the calculation of transition probabilities also provides an effective means for the systematization of cancellation effects that lead to anomalous intensities in alkali-like spectra. The isoelectronic variation of the quantum defects produces differential shifts in phases of the upper and lower state wavefunctions for a given transition. This leads to regular cancellations in the transition integral as a function of effective quantum numbers, $n^* = n - \delta$. If the n^* values for a cancellation nearly coincide with those of a physical ion, an anomalously weak line or anomalous intensity ratios within a multiplet will result. A knowledge of the precise location of these cancellations is valuable both in the classification of spectra and in the study of small perturbations that become measurable when the dominant interaction is absent. A simple graphical technique, based on the quantum defect method, has been developed[15] which uses empirical data to locate likely regions of cancellation. This has permitted comprehensive predictions[15,16] of these near cancellations, some of which have recently been verified in spectroscopic studies for the Cu sequence.[17,18]

THE CORE POLARIZATION MODEL

Nonpenetrating Rydberg states correspond to the high-l yrast[19] and yrare states. For these states the quantum defect approach is valid, but the fitting parameters can be reduced in number and given phenemological interpretation through a simple core polarization model. The effect of the core electrons is assumed to be dominated by long range electrostatic interactions represented by a multipole expansion. The term energy (with an appropriate spinless average over fine

structure levels) is represented by[20]

$$E_\infty - E_{nl} = TH_{nl} + \mathrm{A}\,\langle r^{-4}\rangle_{nl} + \mathrm{B}\,\langle r^{-6}\rangle_{nl} + \ldots . \qquad (3)$$

Here TH_{nl} and $\langle r^{-k}\rangle_{nl}$ are the corresponding term energy and radial expectation values for a level $|nl\rangle$ in a hydrogen-like ion central charge ζ. For an ideally nonpenetrating case $\mathrm{A} = \alpha_d$ and $\mathrm{B} = \alpha_q - 6\beta$, where α_d and α_q are the dipole and quadrupole polarizabilities of the core and β is a nonadiabatic correction for the inability of the core to instantaneously adjust to the motion of the orbital electron. In the reduction of experimental data, usually B and often A are left as fitting parameters. Although this type of expansion does not converge mathematically, penetration effects become increasingly important with higher reciprocal powers of r and tend to quench the physical series. In practice, the series is usually terminated with $\langle r^{-6}\rangle$. This formulation permits the entire nonpenetrating spectrum to be described by the two parameters A and B. If a chain of known transitions connects the nonpenetrating states to the ground state, the ionization potential is also determined.

Consistent with the operational definition of nonpenetrating states ($b_l < 0$) this approach has been utilized very successfully[21] for Rydberg series with $l > 2$ in the Li sequence and with $l > 3$ in the Na sequence. The standard procedure for systems for which excitation energies relative to the ground state are known is to plot the empirical quantity $[E_\infty - E - TH]/\langle r^{-4}\rangle$ vs. $\langle r^{-6}\rangle/\langle r^{-4}\rangle$ for various n and l. For systems for which only relative excitation energies are known, similar plotting variables can be formed using differences. If the representation is successful this plot will yield a straight line of slope B and intercept A. Theoretical calculations of α_d for these inert gas-like ionic cores agree well with empirical values for A deduced from alkali-like spectra.[22] Theoretical calculations are also available[22] for α_φ but no comprehensive predictions for β are available for inert gas-like cores, precluding theoretical comparisons for B. There are, however, indications that penetration effects tend to distort empirical values of B more than those of A.[23]

The method has also been applied to the alkaline earth sequences. Here the polarizabilities are much larger than those of the inert gas cores and arise mainly from the single out-of-shell electron in the

alkali-like core. Thus the individual l components of the transitions between two n shells in an alkaline earth-like ion form well separated and easily recognizable groups of spectral lines. These lines are copiously produced in fast-ion beam spectra and would provide much-needed calibration standards if their wavelengths could be reliably predicted by the polarization model. However, alkali-like cores are much larger than inert gas cores, and penetration effects can be substantial. It now appears that the A and B parameters obtained in earlier spectroscopic analyses that neglected penetration effects for $l > 3$ in the Be sequence and for $l > 4$ in the Mg sequence cannot be directly used to predict states of higher l.

A comprehensive comparison of calculations[24] of α_d and $\alpha_q - 6\beta$ for alkali-like cores with empirical results for A and B deduced from alkaline earth-like spectral data shows that systematically A is about 10% lower than α_d and B differs both in sign and magnitude from $\alpha_q - 6\beta$. This is consistent with the suggestion[23] that penetration effects have an n dependence for fixed l similar to that of $\langle r^{-6} \rangle$, with a proportionality constant that decreases with increasing l. Each

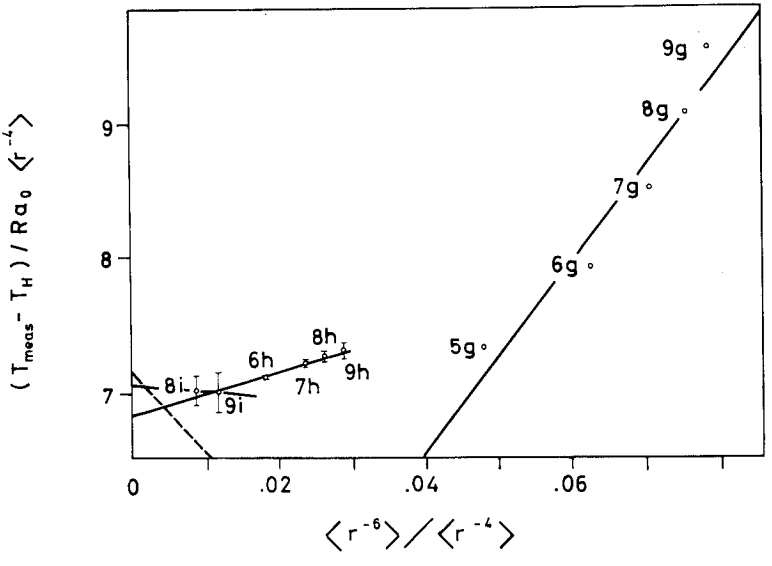

FIGURE 1 Core polarization analysis for Si III. The dashed line indicates the predictions using theoretical values for α_d and α_q-6β and the solid lines denote fits for each series.

individual Rydberg series would then yield α_d as its intercept, but the slope would decrease with l. Figure 1 shows a polarization plot for Si III, with the individual G, H and I Rydberg series separately fitted and compared with the theoretical prediction. Although experimental uncertainties in these sliding spark data become large for high l states, Fig. 1 lends some credence to the interpretation of Ref. 23.

A simple parametrization of these penetration effects has been developed that permits the use of theoretical values for α_d, α_q and β for the in the polarization model to predict high n and l states. Since systematization is the primary goal, simple classical models can be preferable to theoretically justifiable approaches. Thus the core is represented by a simple hollow shell of charge that is penetrated by the orbit. The expectation values $\langle r^{-k} \rangle$ are corrected for the segment of the Keplerian orbit that lies inside the shell and the radius and surface charge are least-squares adjusted to fit the empirical data. Despite its simplicity, this model has reproduced measured term value data[26] to within 1 part in 10^8 and its predictive power is assumed to be of comparable accuracy. Recent experimental breakthroughs provide additional tests of this model of even greater accuracy.

Laser and radiofrequency resonance techniques have provided major advances in the measurement of electrostatic energy intervals. Farley *et al.*[27] and Lundeen and co-workers[28,29] have measured energy separations to within 1 MHz between levels of the same n but different l in neutral helium. The measurements probe directly the relativistic, polarization, and penetration contributions to the energy, exclusive of the much larger l-independent gross (Balmer) energy, providing very stringent tests of the core polarization model and the penetration corrections.

Helium and helium-like atoms provide a unique theoretical case because adiabatic and nonadiabatic polarizabilities of the hydrogen-like core are exactly calculable.[30,31] In addition, a number of subtle corrections have been theoretically proposed that can be tested by the application of the core polarization model to these data. Kelsey and Spruch[32] have suggested that long range interactions in atomic Rydberg states are modified by Casimir–Polder retardation effects. Their computations (verified by Feinberg and Sucher[33]) for asymptotically large r predict two retardation corrections to Eq. (3); one proportional to $\langle r^{-5} \rangle$ and another proportional to $\langle r^{-6} \rangle$. Other contributing effects that have been proposed include: relativistic[34,35] and recoil[31,36] corrections to the dipole polarizability, nonstandard reduced

mass corrections to the relativistic kinetic energy and subtleties in the mixed Z scaling of hydrogenic multipolarities higher than quadrupole.[31]

An analysis of these data has been made[30] using theoretical values for adiabatic and nonadiabatic polarizabilities up to tenth order, with penetration effects parametrized as formulated in Ref. 25. Tests were made of the goodness of fit with various truncations of the multipole series and with various inclusions of other suggested contributing effects. The following conclusions could be drawn: (a) the polarization model with theoretical polarizabilities described the levels with $l \geq 4$ to within a MHz with NO free parameters; (b) inclusion of multipolarities higher than quadrupole worsened the agreement, suggesting a penetration-quenched truncation of series; (c) levels with $l = 2$ and 3 were also described by the use of theoretical polarizabilities with the empirically fitted penetration parameters; and (d) the inclusion of the retardation corrections substantially worsened the agreement.

The failure to observe the retardation effects raises interesting questions. Reference 32 defines by "long range" an orbit for which the round trip core transit time of a virtual photon is comparable to the Keplerian period of the core electron. For a helium atom the period of a $1s$ electron corresponds to the light transit time of the major diameter of an $n = 10$ orbital, precisely the value of n for which the most accurate measurements have been made.[29] This motivates further theoretical study of these effects in the intermediate region of large but finite r. Isoelectronic studies might also be useful in probing these interactions, since the $1s$ orbital period scales with $1/Z^2$, whereas the major axis of the outer orbital scales with $n^2/(Z - 1)$. The present level of accuracy is nearly sufficient to probe the relativistic and recoil contributions to the dipole moment. It is remarkable that this naive semiclassical polarization model should occupy a pivotal role in the testing of sophisticated quantum electrodynamic and relativistic theories.

Recently, Gallagher *et al.*[37] have measured similar $\Delta n = 0$ electrostatic intervals in Ba I, providing another precision test of the penetration parametrization of the polarization model in an alkaline earth system of much greater complexity that He I. Here again an empirical parametrization was performed[38] that was successful in describing the data and in making precise extrapolative predictions. Using theoretical values for $\alpha_q - 6\beta$ and fitted values for α_d and the penetration parameters, the Ba I intervals $6snh$–$6sni$–$6snk$ were

described to within a few MHz for $n = 18$–23. As shown in Table I, the empirical fit yielded an effective $\alpha_d(Ba^+)$ that compares well with a Coulomb approximation estimate, but disagrees with an ab initio Hartree–Slater calculation.

Chang[39] has used the core polarization model to study the Ca I data obtained by Beigang and Wynne[40] and by Vaidyanathan *et al.* [41,42] This enabled him to classify an unidentified line and to extract an effective value for α_d (Ca^+). As shown in Table I, this value also compares more favorably with the Coulomb approximation estimate than with a relativistic Hartree–Fock calculation.

Emission lines from the far infrared solar spectrum are also a source of data which can be systematized by use of the polarization model. Recently the observation of two strong emission lines of this type at 123 183 and 122 207 Å were reported.[43,44] These lines were considered important to astrophysics because they are narrow, have a large Zeeman sensitivity and (unlike most magnetically sensitive visible solar lines) are chromospheric rather than photospheric. Speculations concerning their origin ended when the lines were identified as the $6h$–$7i$ and $6g$–$7h$ transitions in Mg I. Using the core polarization model and the line list presented in Ref. 44, Chang[45] identified these and other similar transitions in both Mg I and Al I and extracted from them the effective values for α_d (Mg^+) and α_d (Al^+). As shown in Table I, here again the empirical value for the alkali-like α_d (Mg^+) compares more favorably with a Coulomb approximation estimate than with ab initio calculations.[46,47] From these studies it is clear that spectral analysis of extraterrestrial sources not only aids in astrophysical interpretation, but also provides a low density light source which populates high n and l states, well described by the core polarization model.

Transition probabilities between nonpenetrating states can also be corrected for core polarizability. The single electron transition moment should properly include both the dipole moment of the valence electron and that induced in the core. A simple means of taking this into account has been formulated.[48]

SCREENING PARAMETRIZATIONS

The quantum defect formulation (which includes the core polarization and penetration model) treats the core region through its modification

of the external portion of the wavefunction. This is not the optimum approach to the description of quantities that are primarily sensitive to the inner portion of the wavefunction. Screening parametrizations provide an alternative empirical framework better suited for the description of such quantities. In a screening parametrization quantum numbers retain their integer values and deviations from the independent particle model are forced to reside in an empirical effective central charge.

The screening parameter approach began with Moseley's parametrization of the Balmer formula to describe x-ray line series and Sommerfeld's relativistic formulation of the x-ray regular doublet law. The approach can also be applied to spin-orbit energies, direct and exchange electron–electron Slater energies, and even to gross energies and transition probabilities. The magnitude and dependence of the screening parameter obtained is, however, very specific to the quantity from which it was extracted.

The regular doublet law is one of the most successful applications of a screening parametrization. It consists of mapping the fine structure separation $\Delta\sigma$ between the levels of maximum and minimum j within a term $|nl>$ into a parameter S, defined by a screened hydrogen-like formula

$$\Delta\sigma = \mathrm{Ry}\,\alpha^2(Z-S)^4/n^3l(l+1) + \text{higher order.} \qquad (4)$$

S varies much less rapidly with Z than does $\Delta\sigma$ and often exhibits regularities that would not have been suspected from the raw data. Experience indicates that the isoelectronic regularity of S for high Z is improved if all higher order contributions that would pertain to a hydrogen-like atom of central charge $Z-S$ are also included in Eq. (4). The higher order terms arising from a Sommerfeld expansion of the Dirac energy are known to arbitrary order[49] and the Z dependence of quantum electrodynamic factors can be represented using the calculations of Mohr.[50] The QED factors were anticipated already in 1923 by Green,[51] who observed that the regularity of the parametrization of x-ray data was improved if an empirical truncation procedure for the high order relativistic terms was followed. In retrospect it is clear that this procedure effectively incorporated a (then

unknown) partial cancellation between relativistic and QED contributions.

It is instructive to compare corresponding levels from characteristic x-ray and highly ionized spectra. The values of S obtained from doublet splittings in x-ray spectra in neutral atoms are nearly constant as a function of Z, showing only slight curvatures and shell structure effects.[52] In contrast, for an optical electron in an isoelectronic sequence the screening decreases with increasing nuclear charge, and is often well represented by the empirical ansatz

$$S = S_0 + S_1/(Z-S) + \ldots . \tag{5}$$

It is well-known that the gross structure of a complex ion approaches fully screened hydrogenic behavior with increasing Z along an isoelectronic sequence. This is often explained classically as a result of differential screening which causes the core to shrink relative to the orbit of the optical electron. Clearly this picture does not describe the fine structure screening, where the orbital electron seems to penetrate more deeply into the core at high Z. Both results can be made classically plausible by imagining a distorted orbit with a perihelion that shrinks faster with Z than the core and an aphelion that shrinks

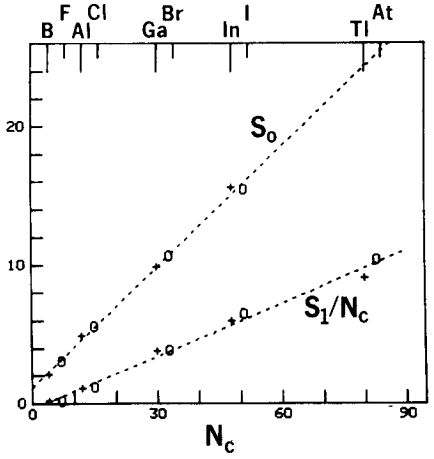

FIGURE 2 Homologous analysis of the screening parameter fitting constants extracted from the $n = 2$–6 ns^2np and ns^2np^5 isoelectronic sequences. The screening constants are plotted vs. an effective number of core electrons defined in the text.

slower with Z than the core. As Z increases, quantities sensitive to the outer wavefunction are increasingly screened and quantities sensitive to the inner wavefunction are decreasingly screened.

The extrapolation of fine structure separations to high stages of ionization has been recently applied to forbidden transitions observed in tokamak plasmas (e.g., Ref. 53). Transitions between two fine structure levels within a term or between two terms within a low lying configuration have diagnostic advantages. They are of much longer wavelengths than other transitions in the same ion, often permitting observation in the spectroscopic air region using lenses and reflective optics. They also have enlarged line profiles and provide information on the thermal Doppler effect.

Examples of systems of this type for which extensive semiempirical extrapolations have been made[54] include the $ns^2np\ ^2P$ ground terms of B, Al, Ga, In, and Tl sequences and the $ns^2np^5\ ^2P$ ground terms in the F, Cl, Br, I, and At sequences. Here values of S_0 and S_1 in Eq. (5) have been obtained for each isoelectronic sequence and studied as a function of n for the homologous sets of sequences. For these sequences the linearity of the parametrization is improved slightly if Ry is replaced by $\mathrm{Ry}/(1 + \epsilon)$, where ϵ is a fitting constant. The fitting parameters S_0 and S_1 extracted from each of these isoelectronic sequences can form a subject for homologous study. By defining an effective number of core electrons N_c such that $N_c(ns^2np) = N - 1$ and $N_c(ns^2np^5) = N = 2$, an interesting trend emerges. Figure 2 displays a plot of S_0 and S_1/N_c versus N_c, and indicates that these isoelectronic quantities are not only linear, but that both homologous sequences are described by the same straight lines. Thus four parameters (two slopes and two intercepts on Fig. 2) describe the ground term fine structures of all members of ten isoelectronic sequences. For $Z \leq 92$ this corresponds to 552 different ions. Extrapolated accuracies are difficult to judge, but interpolated accuracies are generally within a few parts in 10^4. A study[55] has been made of the $4s^24p\ ^2P$ fine structure splitting in the Ga sequence that utilized tokamak plasma, laser-produced plasma and low-inductance vacuum spark measurements to verify and extend this semiempirical formulation, as well as to correct earlier misclassifications.

Assuming nonrelativistic j-independent wavefunctions, the $M1$ intraterm transition probability is independent of radial operators, and depends only on angular momentum factors and the cube of the transition wavelength[56] (multiconfiguration Hartree–Fock and Dirac–

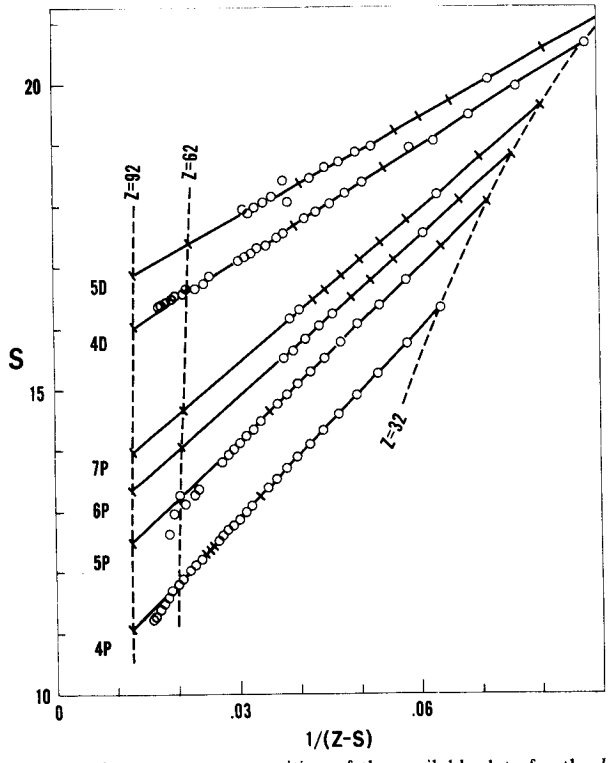

FIGURE 3 Screening parameter exposition of the available data for the $l = 1$ and 2 fine structure separations in the Cu isoelectronic sequence.

Fock calculations substantiate this assumption). Thus the screening parametrization provides both the wavelength and the lifetime for these transitions.

The most comprehensive base of isoelectronic fine structure data[18,58,59] (cf. Ref. 57) presently available is that of the Cu sequence. For this system fine structure separations have been studied through 46 stages of ionization for the $4p$, $5p$, $6p$, $4d$, and $5d$ terms. Screening parametrization studies[57] have been made for each of these splittings. Figure 3 presents an exposition of the data base as a plot of S vs. $1/(Z-S)$ and the empirical regularities are manifest. Notice that for a given l the slope decreases and the intercept increases with increasing n. This has been quantitatively formulated[57] and permits the prediction of fine structures for higher members of the ^2P and ^2D

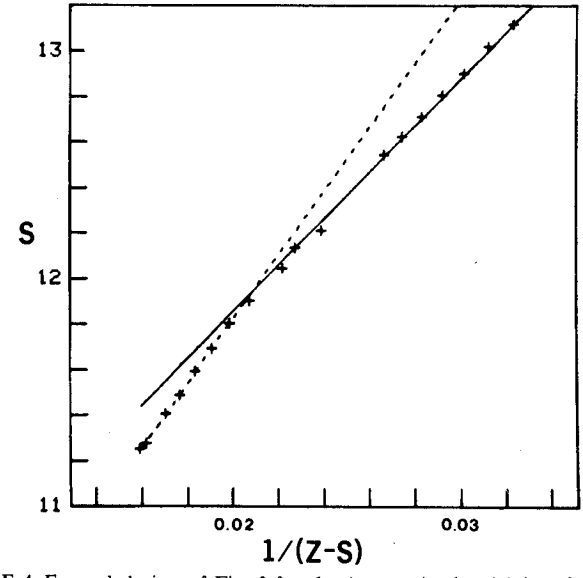

FIGURE 4 Expanded view of Fig. 3 for the $4p$ term in the vicinity of $Z = 60$.

Rydberg series for any stage of ionization.

The linearity of the plot persists for all Z for the ^2D states, but for the ^2P states there is slight downward break in the slope at high Z. This is illustrated by Fig. 4, which is an enlargement of the high Z region for the $4p$ term. The data can be represented by two separate straight line fits, with a very sharp break at $Z = 60$. Dirac–Fock calculations[60] predict the fine structure at high Z to accuracies within better than 1%, but exhibit a gentle isoelectronic curvature on this plot with neither a linear region nor a break in the slope. The linearities in Fig. 4 permit predictions to 1 part in 10^4, but their origin is unclear.

The lack of a theoretical explanation for the break in slope in Fig. 4 has motivated a semiclassical self-consistent field calculation[61] for this system. Each orbit was required to satisfy the Bohr–Sommerfeld–Wilson quantization rule (as modernized by Einstein–Brillouin–Keller theory and the Maslov topological index) in the field deduced from their composite classical probability densities. When the relativistic version of the Hamilton–Jacobi formulation was used, two classical occurrences in the vicinity of $Z = 60$ for the Cu sequence

emerged: (1) the 1*s* aphelion crosses the perihelions of the *np* Rydberg series and; (2) the small but finite perihelion of the *s* states brought about by the classical Langer modification $[l(l+1) \rightarrow (l+\frac{1}{2})^2]$ collapses for $2\alpha Z > 1$. These results are intriguing, but it remains to be seen whether quantum mechanical counterparts to these semiclassical charge redistributions can be found.

Screening parametrizations are not limited to the spin-orbit interaction, but can also be applied to the electron–electron direct and exchange Slater integrals. Terms of the form $nsnp\ ^{1,3}P$ in the Mg, Zn, Cd, and Hg sequences are well suited to this parametrization, since both two out-of-core electrons are in the same shell and are empirically representable by the same screening constant. Complete sets of observations up to high stages of ionization have recently become available for the $ns^2\ ^1S_0$–$nsnp\ ^1P_1$ resonance transitions in the[62] Mg and[63] Zn isoelectronic sequences. Tokamak and laser-produced plasma studies (cf. Refs. 64, 65) have provided some measurements of the $ns^2\ ^1S_0$–$nsnp\ ^3P_1$ intercombination lines and the $M1$ $nsnp\ ^3P_2$–$^3P_1$ and the $E2$ $nsnp\ ^3P_2$–$^3P_0$ intraterm lines and motivate a systematization of the data.

Relative to the singlet excitation energy, the triplet energies are functions of the spin-orbit energy $\Delta\sigma$ and the exchange Slater integral

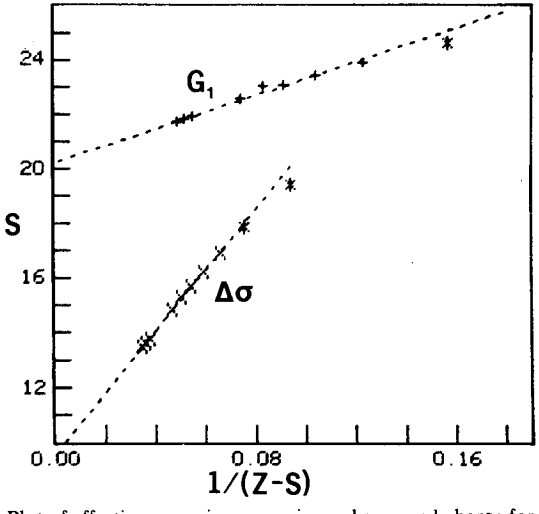

FIGURE 5 Plot of effective screening vs. reciprocal screened charge for the exchange Slater energy G_1 and the spin-orbit energy $\Delta\sigma$ for the Zn isoelectronic sequence.

G_1. $\Delta\sigma$ can again be parametrized using Eqs. (4) and (5). A screening parametrization of G_1 can be obtained using screened hydrogen-like wavefunctions, which yield values $G_1 = 15\ \mathrm{Ry}(Z\text{–}S)/256$ for $n = 3$ and $G_1 = 65\ \mathrm{Ry}(Z\text{–}S)/2304$ for $n = 4$. The G_1 screening parameter defined in this manner seems also to be nearly linear as a function of $1/(Z\text{–}S)$. Plots of the screening parameters for the spin-orbit and exchange Slater integrals for the Zn sequence are shown in Fig. 5. Semiempirical systematizations of the[64] Mg and[66] Zn isoelectronic sequences and extrapolative predictions have been made utilizing these linearities. Measurements for the Cd sequence[67] have recently become available, and show a similar trend. Extrapolation of these results yields predictions characteristic Cd-like lines in lanthanide ions, which would provide a much less complicated spectrum than is normally associated with these elements.

CONCLUSION

The use of semiempirical methods can provide a comprehensive systematization of large blocks of data. Through the recognition of regularities, all of the data in a block can be utilized to produce a set of values which are more accurate than any single measurement in the block. Interpolative and extrapolative predictions can be made with a precision comparable to that of the data base available. Historically, the regularities revealed by empirical studies have played a crucial role in the development of fundamental theory and calculational methods. Similarly, some of the empirical regularities described here may contain clues to an improved understanding of the dynamics of complex atoms.

Acknowledgments

This work was partially supported by the U.S. Department of Energy, Division of Chemical Sciences, under Contract No. DE-AS05-80ER10676.

LORENZO J. CURTIS

Department of Physics and Astronomy,
University of Toledo,
Toledo, Ohio 43606

References

1. B. Edlén, Hand. Physik **27**, 80 (1964).
2. C. Fabre and S. Haroche, in *Rydberg States of Atoms and Molecules*, edited by R. F. Stebbings and F. B. Dunning (Cambridge University Press, Cambridge, 1983), pp. 117–164.
3. C. Jaffé and W. P. Reinhardt, J. Chem. Phys. **66**, 1285 (1977).
4. L. J. Curtis, Nucl. Instr. Meth. **202**, 333 (1981).
5. C. J. Lorenzen, K.-H. Weber, and K. Niemax, Opt. Commun. **33**, 271 (1980).
6. L. R. Pendrill, D. Delande, and J. C. Gay, J. Phys. B **12**, L603 (1979).
7. A. Pedlar and R. D. Davies, in *Radio Recombination Lines*, edited by P. A. Shaver (Reidel, Holland, 1980), p. 239.
8. D. Kleppner, M. G. Littman, and M. L. Zimmerman, *Rydberg States of Atoms and Molecules*, edited by R. F. Stebbings and F. B. Dunning (Cambridge University Press, Cambridge, 1983), pp. 73–116.
9. F. H. Read, J. Phys. B **10**, 449 (1977).
10. Cf. e.g., U. Fano, Comments Atom. Molec. Phys. **10**, 223 (1981); M. J. Seaton, Comments Atom. Molec. Phys. **2**, 37 (1970).
11. K. T. Lu and U. Fano, Phys. Rev. A **2**, 81 (1970).
12. A. Lindgård and S. E. Nielsen, Atomic Data Nucl. Data Tables **19**, 533 (1977).
13. A. Gaupp, P. Kuske, and H. J. Andrä, Phys. Rev. A **26**, 3351 (1982).
14. R. P. McEachran and M. Cohen, J. Phys. B **16**, 3125 (1983).
15. L. J. Curtis and D. G. Ellis, J. Phys. B **11**, L543 (1978); **13**, L431 (1980).
16. L. J. Curtis, J. Opt. Soc. Am. **71**, 566 (1981).
17. N. Acquista and J. Reader, J. Opt. Soc. Am. **71**, 569 (1981).
18. J. Reader, S. Goldsmith, and N. Acquista, J. Opt. Soc. Am. (in press).
19. J. R. Grover, Phys. Rev. **157**, 832 (1967).
20. References to the historical development of the polarization model are given by K. Bockasten, Phys. Rev. **102**, 729 (1956).
21. B. Edlén, Physica Scripta **19**, 225 (1979); **17**, 564 (1978).
22. W. R. Johnson, D. Kolb, and K.-N. Huang, Atomic Data Nucl. Data Tables **28**, 333 (1983).
23. P. Vogel, Nucl. Instr. Meth. **110**, 241 (1973).
24. L. J. Curtis, Physica Scripta **21**, 162 (1980); Phys. Rev. A **23**, 362 (1981).
25. L. J. Curtis, J. Phys. B **14**, 1373 (1981).
26. L. J. Curtis and P. S. Ramanujam, J. Opt. Soc. Am. **71**, 1315 (1981).
27. J. W. Farley, K. B. MacAdam, and W. H. Wing, Phys. Rev. A **20**, 1754 (1979).
28. D. R. Cok and S. R. Lundeen, Phys. Rev. A **23**, 2488 (1981); **24**, 3283(E) (1981).
29. S. L. Palfrey and S. R. Lundeen, Phys. Rev. A (in press).
30. L. J. Curtis and P. S. Ramanujam, Phys. Rev. A **25**, 3090 (1982).
31. R. J. Drachman, Phys. Rev. A **26**, 1228 (1983).
32. E. J. Kelsey and L. Spruch, Phys. Rev. A **18**, 15; 845; 1055 (1978).
33. G. Feinberg and J. Sucher, Phys. Rev. A **27**, 1958 (1983).
34. G. W. F. Drake and S. P. Goldman, Phys. Rev. A **23**, 2093 (1981).
35. B. A. Zon, N. L. Manakov, and L. P. Rapoport, Sov. J. Nucl. Phys. **15**, 282 (1972).
36. M. Martinis and H. Pilkuhn, J. Phys. B **15**, 1797 (1982).
37. T. F. Gallagher, R. Kachru, and N. H. Tran, Phys. Rev. A **26**, 2611 (1982).
38. L. J. Curtis, P. S. Ramanujam, and C. E. Theodosiou, Phys. Rev. A **28**, 1151 (1983).
39. E. S. Chang, J. Phys. B **16**, L539 (1983).
40. R. Beigang and J. J. Wynne, Optics Lett. **6**, 295 (1981).

41. A. G. Vaidyanathan, W. P. Spencer, J. R. Rubbmark, H. Kuiper, C. Fabre, D. Kleppner, and T. W. Ducas, Phys. Rev. A **26**, 3346 (1982).
42. A. G. Vaidyanathan and P. Shorer, Phys. Rev. A **25**, 3108 (1982).
43. F. J. Murcray, A. Goldman, F. H. Murcray, C. M. Bradford, D. G. Murcray, M. T. Coffey, and W. G. Mankin, Ap. J. **247**, L97 (1981).
44. J. Brault and R. Noyes, Ap. J. **269**, L61 (1983).
45. E. S. Chang and R. W. Noyes, Ap. J. **275**, L11 (1983).
46. S. I. Easa and G. C. Shukla, J. Physique **40**, 137 (1979).
47. P. W. Langhoff and R. P. Hurst, Phys. Rev. **139**, A1415 (1965).
48. L. J. Curtis, J. Phys. B **12**, L509 (1979).
49. L. J. Curtis, J. Phys. B **10**, L641 (1977).
50. P. J. Mohr, Phys. Rev. A **26**, 2338 (1982).
51. J. B. Green, Phys. Rev. **21**, 397 (1923).
52. A. F. Burr and J. K. Carson, J. Phys. B **7**, 451 (1974).
53. B. Denne, E. Hinnov, S. Suckewer, and S. Cohen, Phys. Rev. A **28**, 206 (1983).
54. L. J. Curtis and P. S. Ramanujam, Phys. Rev. A **26**, 3627 (1982); Physica Scripta **27**, 417 (1983).
55. L. J. Curtis, J. Reader, S. Goldsmith, B. Denne, and E. Hinnov, Phys. Rev. A **29**, 2248 (1984).
56. L. J. Curtis, Phys. Scripta (in press).
57. L. J. Curtis, J. Phys. B **14**, 631 (1981).
58. J. Reader and G. Luther, Phys. Scripta **24**, 732 (1981).
59. J. Reader, N. Acquista, and D. Cooper, J. Opt. Soc. Am. **73**, 1765 (1983).
60. K.-T. Cheng and Y.-K. Kim, Atom. Data Nucl. Data Tables **22**, 547 (1978).
61. L. J. Curtis and R. R. Silbar, J. Phys. B (in press).
62. J. Reader, J. Opt. Soc. Am. **73**, 796 (1983).
63. N. Acquista and J. Reader, J. Opt. Soc. Am. (in press).
64. L. J. Curtis and P. S. Ramanujam, J. Opt. Soc. Am. **73**, 979 (1983).
65. U. Litzén and K. Ando, Phys. Lett. A **100**, 411 (1984).
66. L. J. Curtis, *Atomic Spectroscopy Annual Report 1983* (University of Lund, Lund, Sweden) pp. 58–61.
67. V. Kaufman, personal communication.